Circulation: Arrhythmia and Electrophysiology

ORIGINAL ARTICLE

# Genetic Loss of $I_{K1}$ Causes Adrenergic-Induced Phase 3 Early Afterdepolariz ations and Polymorphic and Bidirectional Ventricular Tachycardia

Louise Reilly, PhD; Francisco J. Alvarado, PhD; Di Lang, PhD; Sara Abozeid, BS; Hannah Van Ert, BS; Cordell Spellman, BS; Jarrett Warden, BS; Jonathan C. Makielski, MD; Alexey V. Glukhov, PhD; Lee L. Eckhardt, MD

**BACKGROUND:** Arrhythmia syndromes associated with *KCNJ2* mutations have been described clinically; however, little is known of the underlying arrhythmia mechanism. We create the first patient inspired *KCNJ2* transgenic mouse and study effects of this mutation on cardiac function, $I_{K1}$, and $Ca^{2+}$ handling, to determine the underlying cellular arrhythmic pathogenesis.

**METHODS:** A cardiac-specific *KCNJ2*-R67Q mouse was generated and bred for heterozygosity (R67Q$^{+/-}$). Echocardiography was performed at rest, under anesthesia. In vivo ECG recording and whole heart optical mapping of intact hearts was performed before and after adrenergic stimulation in wild-type (WT) littermate controls and R67Q$^{+/-}$ mice. $I_{K1}$ measurements, action potential characterization, and intracellular $Ca^{2+}$ imaging from isolated ventricular myocytes at baseline and after adrenergic stimulation were performed in WT and R67Q$^{+/-}$ mice.

**RESULTS:** R67Q$^{+/-}$ mice (n=17) showed normal cardiac function, structure, and baseline electrical activity compared with WT (n=10). Following epinephrine and caffeine, only the R67Q$^{+/-}$ mice had bidirectional ventricular tachycardia, ventricular tachycardia, frequent ventricular ectopy, and/or bigeminy and optical mapping demonstrated high prevalence of spontaneous and sustained ventricular arrhythmia. Both R67Q$^{+/-}$ (n=8) and WT myocytes (n=9) demonstrated typical n-shaped $I_{K1}$ *IV* relationship; however, following isoproterenol, max outward $I_{K1}$ increased by ≈20% in WT but decreased by ≈24% in R67Q$^{+/-}$ ($P$<0.01). R67Q$^{+/-}$ myocytes (n=5) demonstrated prolonged action potential duration at 90% repolarization and after 10 nmol/L isoproterenol compared with WT (n=7; $P$<0.05). $Ca^{2+}$ transient amplitude, 50% decay rate, and sarcoplasmic reticulum $Ca^{2+}$ content were not different between WT (n=18) and R67Q$^{+/-}$ (n=16) myocytes. R67Q$^{+/-}$ myocytes (n=10) under adrenergic stimulation showed frequent spontaneous development of early afterdepolarizations that occurred at phase 3 of action potential repolarization.

**CONCLUSIONS:** *KCNJ2* mutation R67Q$^{+/-}$ causes adrenergic-dependent loss of $I_{K1}$ during terminal repolarization and vulnerability to phase 3 early afterdepolarizations. This model clarifies a heretofore unknown arrhythmia mechanism and extends our understanding of treatment implications for patients with *KCNJ2* mutation.

**GRAPHIC ABSTRACT:** A graphic abstract is available for this article.

**Key Words:** action potential ■ heart ■ potassium channels ■ sarcoplasmic reticulum ■ tachycardia, ventricular

Human cardiac myocyte electrical stability depends on normal polarization of the resting potential achieved by the inward-rectifier $K^+$ current ($I_{K1}$). *KCNJ2* encodes for the pore-forming subunit Kir2.1 and creates the dominant component for $I_{K1}$ that functions to maintain the resting membrane potential, completes phase 3 repolarization, and indirectly determines cellular excitability.[1,2] Four different arrhythmia syndromes based on clinical phenotype have been associated with *KCNJ2* mutations: Anderson-Tawil Syndrome,[3] short QT

Correspondence to: Lee L. Eckhardt, MD, 8431 Wisconsin Institute for Medical Research (WIMR2), 1111 Highland Ave, Madison, WI 53705. Email lle@medicine.wisc.edu
The Data Supplement is available at https://www.ahajournals.org/doi/suppl/10.1161/CIRCEP.120.008638.
For Sources of Funding and Disclosures, see page 979.

*Circulation: Arrhythmia and Electrophysiology* is available at www.ahajournals.org/journal/circep

## WHAT IS KNOWN?

- Mutations in *KCNJ2* can result in a variety of phenotypic presentations, but the arrhythmia mechanism(s) remain unknown.

## WHAT THE STUDY ADDS?

- We created the first patient-inspired *KCNJ2* in vivo model from a patient missense mutation and presented with catecholaminergic polymorphic ventricular tachycardia-like phenotype.
- *KCNJ2* in vivo model demonstrates aggressive ventricular arrhythmia including frequent bidirectional ventricular tachycardia similar to the patient.
- The arrhythmia mechanism depends not on abnormal calcium handling (as in catecholaminergic polymorphic ventricular tachycardia) but adrenergic loss of $I_{K1}$ causing phase 3 early afterdepolarizations.
- This in vivo model demonstrates a unique arrhythmia mechanism and highlights the complexity of *KCNJ2* mutation-related arrhythmia syndromes as well as phenotypic categorization.

## Nonstandard Abbreviations and Acronyms

| | |
|---|---|
| **AP** | action potential |
| **APD** | action potential duration |
| **ATS** | Anderson-Tawil Syndrome |
| **BiVT** | bidirectional ventricular tachycardia |
| **CaT** | calcium transient |
| **CPVT** | catecholaminergic polymorphic ventricular tachycardia |
| **DAD** | delayed afterdepolarization |
| **EAD** | early afterdepolarization |
| **$I_{K1}$** | inward-rectifier $K^+$ current |
| **IP** | intraperitoneal |
| **LV** | left ventricular |
| **NCX1** | $Na^+/Ca^{2+}$-exchanger |
| **PMVT** | polymorphic ventricular tachycardia |
| **RV** | right ventricular |
| **SR** | sarcoplasmic reticulum |
| **VT** | ventricular tachycardia |
| **WT** | wild-type |

syndrome 3,[4] familial atrial fibrillation,[5] and catecholaminergic polymorphic ventricular tachycardia (CPVT).[6] The cellular correlate to Kir2.1 dysfunction for Anderson-Tawil Syndrome is a loss of function, while short QT syndrome 3 and Familial Atrial Fibrillation are thought to be because of a gain of function.[5,7] Moreover, some *KCNJ2* mutations have been clinically described in patient cohorts presenting with a CPVT-like phenotype, yet the cellular correlates have not been clarified. Unraveling the arrhythmia mechanism related to *KCNJ2* mutations has been hindered by the lack of transgenic in vivo models. Prior investigation of *KCNJ2* mutation syndromes has been limited to heterologous expression of mutations or employed the use of Kir2.1 blockers to mimic the cellular effects.[8,9] Such approaches underestimate more complex channel regulation, and important subcellular interactions may be misunderstood by reducing the mutation effect to a gain or loss of function. For example, we found that certain *KCNJ2* mutations can influence the rectification index with a preferential effect of loss of outward (physiological) $I_{K1}$.[10]

We previously reported a patient who harbors *KCNJ2* mutation, R67Q, and presented with exertion-induced polymorphic ventricular tachycardia (PMVT), bidirectional ventricular tachycardia (BiVT), and syncope,[11] a similar phenotype to CPVT.[12] Arrhythmia in CPVT is related to altered intracellular calcium $[Ca^{2+}]_i$ handling leading to a propensity to develop delayed afterdepolarizations (DADs) and genetically linked to mutations in the cardiac ryanodine receptor (*RYR2*),[13] and calsequestrin-2 (*CASQ2*).[14] Additionally, patients presenting with a CPVT-like phenotype have been noted in association with mutations in triadin (*TRDN*), ankyrin-B (*ANK2*), calmodulin (*CALM1*),[15] and Kir2.1 (*KCNJ2*).[6,16–18] It remains unclear if CPVT-mimicking phenotypes share the same arrhythmia mechanism as *RYR2* or *CASQ2* mutations.[19,20] In a pharmacological-induced loss of $I_{K1}$ in a heart failure rabbit model, loss of Kir2.1 function has been linked to $Ca^{2+}$ overload arrhythmia related to $V_m/Ca_i$ imbalance causing DADs.[21] In contrast to this, in a drug-induced long QT model, loss of $I_{K1}$ was shown to underlie the mechanism for phase 3 early afterdepolarizations (EADs).[22] These studies highlight that the clinical presentation may not mirror the arrhythmia mechanism; discerning these subtleties is important for effective arrhythmia suppression as the treatment approach toward DAD versus EAD suppression is divergent. Unfortunately, the current strategy of extrapolating from diseases with a similar phenotype may result in inaccurate treatment and exposing patients to an increased risk of sudden cardiac death.[23]

It is with this premise that we undertook the creation and characterization of the arrhythmia mechanism in a cardiac-specific knock-in in vivo model inspired by our patient presenting with a CPVT-like phenotype and a *KCNJ2* mutation.[11] Together, these data not only link the clinical arrhythmia presentation with the *KCNJ2* mutation R67Q but may help inform clinical treatment approaches.

## METHODS

The authors declare that all supporting data are available within the article and its Data Supplement. Mouse lines are available from The Jackson Laboratory Model Repository.

## Human Subjects and Animal Use Assurances

The University of Wisconsin Institutional Review Board approved this research in accordance with the National Institutes of Health guidelines for human research. All animal procedures were performed in accordance with the Guide for the Care and Use of Laboratory Animals (National Institutes of Health) and approved by the University of Wisconsin-Madison Institutional Animal Care and Use Committee.

## Cardiac-Specific Knock-In Mice

Cardiac specific knock-in mice were generated in collaboration with University of Wisconsin-Madison Biotechnology Center using the Cre-loxP system.[24] Because of the extracardiac effects of Kir2.1 in development,[25] a cardiac specific knock-in was designed to avoid effects of mal-development on the whole animal and to focus on the patient's arrhythmic phenotype which occurs in absence of extra-cardiac effects. For gene targeting, *Hin*dIII-linearized PL253 targeting vector DNA containing R67Q-*KCNJ2* was electroporated into embryonic stem cells.[26] The target vector contained R67Q-*KCNJ2* with a neocassette inserted into the primary sequence, flanked with loxP sites. This results in silencing of R67Q-*KCNJ2* in tissues that do not express Cre recombinase. To generate the cardiac-specific knock-in, resultant targeted mice were crossed with mice expressing Cre recombinase under the control of the myosin heavy chain 6 promoter (*MYHC6)* to excise the neocassette (B6.FVB-Tg(Myh6-cre)2182Mds/J, Jax stock: #011038(4)). Embryonic stem cells were plated in 100-mm dishes and were cultured for 48 hours. Positive and negative selections were performed using Geneticin (G418) and neomycin, respectively. Positive clones were isolated and confirmed by Southern blot using an external probe to the target sequence and microinjected into the pronucleus of C57BL/6J one-cell mouse embryos. Following microinjections, embryos were transferred into pseudo-pregnant recipients and pups born (University of Wisconsin-Madison Biotechnology Center). Chimeric mice were bred to C57BL/6 mice to establish a hybrid line for 10 generations. Germ-line transmission has generated KCNJ2$^{+}$/KCNJ2$^{R67Q\text{-}neo}$ mice with genetic background 129SV/J from embryonic stem cells and C57BL/6 from blastocysts. Genotypes from F1 and F2 generations were determined by polymerase chain reaction on DNA from ear and tail biopsy specimens. Cardiac-specific transgenic mice were generated by crossing KCNJ2$^{+}$/KCNJ2$^{R67Q\text{-}neo}$ mice with mice obtained from The Jackson Laboratory expressing Cre cDNA under the control of the mouse α-MHC promoter (Tg(Myh6-cre)1Jmk/J, JAX stock #009074). The genotypes from the F1 generation without the neocassette were determined by polymerase chain reaction on DNA from ear, tail biopsy as well as cardiac specimens to ensure the neocassette had been excised. Age-matched male and female littermates (8–12 weeks) wild-type (WT; Cre$^{+}$/R67Q$^{-/-}$ mice are designated WT for the purposes of this study) and heterozygous R67Q (Cre$^{+}$/R67Q$^{+/-}$) were used in whole animal physiological studies (N=8), biochemistry (N=4), whole-cell patch clamp electrophysiology ($I_{K1}$; N=5, n=9 WT, N=5, n=8 for R67Q$^{+/-}$; action potentials [APs]; WT–N=4, n=7; WT+isoproterenol–N=4, n=6; R67Q$^{+/-}$ and R67Q$^{+/-}$+isoproterenol–N=3, n=5) and calcium transient (CaT) studies (line scan CaTs–WT–N4, n=18; R67Q$^{+/-}$–N=4, n=16; Ratiometric CaTs–WT–N=6, n=7; R67Q$^{+/-}$–N=4, n=10).

## Echocardiography

Transthoracic echocardiography was performed on 8- to 12-week-old age mice under 1% isoflurane gas anesthesia using a Visual Sonics 770 ultrasonograph with a 30-MHz transducer (RMV 707B; Visual Sonics, Toronto).[27] Two-dimensionally guided M-mode images were acquired in the long axis. Left ventricular (LV) mass-to-body weight ratio (LV), LV volume during diastole and systole, heart rate, LV dimension in diastole, thickness of the posterior walls in diastole were recorded. Parameters were measured over at least 3 consecutive cycles. Following measurements, mice were sacrificed, and hearts snap-frozen for biochemical analyses. LV mass was calculated using the following equation; LV mass=[1.05×((Posterior $\text{Wall}_{\text{diastole}}$+Anterior $\text{Wall}_{\text{diastole}}$+LV $\text{diameter}_{\text{diastole}}$)3–(LV $\text{diameter}_{\text{diastole}}$)3)].

## Electrocardiography

Adult (8–12 weeks) WT and R67Q$^{+/-}$ mice were anesthetized by 2% isoflurane inhalation and maintained at 1% to 2% for the duration of the measurements. Mice were placed on the monitor (Indus Rodent Surgical Monitor, Indus Instruments, Portland, OR) in the dorsal position and baseline ECGs (Notocord) recorded for 5 minutes. A single induction for arrhythmia initiation was performed with an I.P. injection of caffeine (120 mg/kg) and epinephrine (2 mg/kg). ECG examples were taken 10 minutes following injection. Following cessation of ECG recordings, mice were euthanized, and hearts excised for cardiac genotyping.[28] ECGs were analyzed blinded to animal genotype in accordance with standard protocols. Arrhythmic events were calculated as follows; ECGs were examined for each animal following injection of caffeine and epinephrine and recorded if arrhythmia phenomenon were observed. The number of mice with arrhythmic events for each group was divided by the total number of mice investigated to give an overall percentage of arrhythmic events for each group.

## Isolated Right Ventricular Myocytes

Calcium tolerant myocytes were isolated from the right ventricular (RV) free wall of adult WT and R67Q$^{+/-}$ male and female mice of 8 to 12 weeks in age by perfusion of collagenase II (Worthington Labs) or Liberase (Roche) in the Langendorff model.[29] Mice were anesthetized prior with 5% isoflurane before cardiac excision. Anesthesia was confirmed by absence of response to stimuli (firm toe pinch). Because of known regional variation in $I_{K1}$ within the left ventricular chamber including transmural differences, the RV free wall was selected because of the homogeneity of $I_{K1}$ known to occur in the chamber to create a robust and reproducible dataset. These myocytes were used for cellular electrophysiology and for CaT measurements.

## Cellular Electrophysiology

Electrophysiology experiments were performed using an Axopatch 200B amplifier and pCLAMP10 (Molecular Devices, Sunnyvale, CA). All electrophysiology recordings were performed blinded to the animal genotype.

Voltage clamp data were recorded at room temperature from isolated calcium tolerant adult myocytes from WT and

R67Q$^{+/-}$ mice using whole cell technique.[30] Borosilicate glass pipettes were pulled to resistances of 2 to 3 MΩ when filled (Model P-97, Sutter Instruments, Novato, CA). Bath solution for $I_{K1}$ measurements contained (mM): NaCl 148, KCl 5.4, $CaCl_2$ 1.8, $MgCl_2$ 1, HEPES 15, $NaHPO_4$ 0.4, D-glucose 5.5, and pH adjusted to 7.4 (NaOH). Calcium currents and calcium-sensitive chloride currents were blocked with nifedipine (10 μM) in the bath solution. Pipette filling solution contained (mM): K-gluconate 150, EGTA 5, MgATP 5, HEPES 10 and pH adjusted to 7.2 (KOH). $I_{K1}$ was recorded from a holding potential of −50 mV sequential 10 mV steps from −120 mV to +50 mV in 100 ms steps. This was repeated in the presence of isoproterenol (10 nmol/L). Finally, cells were perfused with bath solution containing 0.5 mmol/L barium chloride and I-V protocol repeated (Figure III in the Data Supplement). This was then subtracted from previously recorded I-V protocols in addition to measuring I-V relationships at 500 ms of protocol to eliminate possible contaminating currents. Cell stability was ensured by recording using the aforementioned protocol twice at baseline, twice following isoproterenol, and twice following barium to ensure consistency. If the cell is unstable or a seal of 250 MΩ is not achieved, then the cell is discarded and another selected and the process repeated. Rectification index was calculated as follows: This index was defined as the ratio of the outward current at −50 mV divided by the absolute value of the inward current at −100 mV and then multiplied by 100.[11]

APs were recorded under current clamp mode at 34±2°C. Myocytes were paced 2 to 6 Hz with a brief depolarizing square pulse using an analog programmable stimulator (Multichannel Systems, Reutlingen, Germany). AP amplitude and upstroke velocity ($dV/dt_{max}$), resting membrane potential, and action potential duration (APD) at 10% ($APD_{10}$), 50% ($APD_{50}$), 70% ($APD_{70}$), and 90% ($APD_{90}$) of repolarization were analyzed (pCLAMP 10). Each myocyte was paced for >100 beats before analysis. The terminal 5 consecutive APs at each frequency (2–6 Hz) were used for analysis. APs were measured at baseline and following incubation with isoproterenol (10 nmol/L). Bath solution for AP was the same as for $I_{K1}$ minus nifedipine and pipette solution contained (mM): KCl 150, NaCl 5, $CaCl_2$ 2, EGTA 5, MgATP 5, HEPES 10, and pH adjusted to 7.2 (KOH).

## Optical Mapping

Male and female mice age 8 to 12 weeks were anesthetized using Isoflurane. Heparin (100 units) was used to treat and prevent blood clots in the veins and arteries. After a midsternal incision, the heart was removed, cannulated, and washed in oxygenated (95% $O_2$ to 5% $CO_2$) constant-temperature (37±1°C) modified Tyrode solution (in mM: 128.2 NaCl, 4.7 KCl, 1.19 $NaH_2PO_4$, 1.05 $MgCl_2$, 1.8 $CaCl_2$, 20.0 $NaHCO_3$, and 11.1 glucose [pH 7.35±0.05]). Perfusion was performed using a peristaltic pump (Peri-Star, WPI, Sarasota, FL) under constant aortic pressure of 60 to 80 mm Hg as measured by a pressure amplifier. Coronary perfused hearts were stained by perfusion with voltage-sensitive dye (RH-237, Invitrogen [Carlsbad, CA], 5 μL of 1 mg/mL DMSO in Tyrode solution] for 5 to 7 minutes. The excitation-contraction uncoupler blebbistatin (10 μM, Tocris Bioscience) was used to prevent the effect of motion artifacts. The fluorescent signals emitted from the preparation was long pass (>700 nm) filtered using an edge pass filter (Thorlabs) before reaching the camera. Emitted signals were directed toward a MiCAM Ultima-L CMOS camera (SciMedia) with high spatial (100×100 pixels, 230±20 μm/pixel) and temporal (500–1000 frames/second) resolution. The acquired fluorescent signal was digitized, amplified, and visualized by custom software (SciMedia).

## Confocal $Ca^{2+}$ Imaging

Following $Ca^{2+}$ re-introduction, myocytes were incubated in 10 μmol/L fluo-4 AM (ThermoFisher) and 0.4% Pluronic F-127 (ThermoFisher) for 5 minutes at 37°C. Then, they were plated on glass-bottom dishes (MatTek) coated with laminin (ThermoFisher) in normal Tyrode solution, containing (mM) 135 NaCl, 4 KCl, 1 $MgCl_2$ 10 HEPES, 1.2 $NaH_2PO_4$, 10 Glucose, and 1.8 $CaCl_2$, pH 7.40 with NaOH. Confocal line-scans were collected with a Zeiss LSM800 microscope using a 40×/1.2 water-immersion objective, at 488 nm excitation and >505 nm emission wavelengths. A 512-pixel line was drawn across the long axis of the cell, and unidirectional line-scans were obtained at 2.47 ms/line. $Ca^{2+}$ transients were elicited through field stimulation using a Grass stimulator (2 ms pulses, 60–70 V) controlled with a model 3800 Stimulator (A-M Systems). The protocol consisted of 5 seconds of rest, 30 seconds at 1 Hz, 15 seconds at 2 Hz, and 15 seconds at 3 Hz, followed by a pulse of 10 mmol/L caffeine to measure sarcoplasmic reticulum (SR) content. Recordings were made in basal conditions and in the presence of 300 nmol/L (−)-isoproterenol. Images were analyzed using a custom-made Matlab 2019b script to calculate the transient amplitude, 50% decay time and maximum $Ca^{2+}$ release velocity ($dF/dt_{MAX}$). $F_0$ was determined as the basal fluorescence during the resting period.

## Ratiometric CaTs

Calcium tolerant RV myocytes were loaded with fura2-AM ratiometric dye (Sigma, St. Louis, MO) at room temperature. CaTs were recorded at 34±2°C using IonOptix Calcium and Contractility System equipped with a Hyperswitch and MyoCam-S (IonOptix, Westwood, MA). Myocytes were paced 2 to 6 Hz with field pacing using Myopacer (IonOptix, Westwood, MA). Bath solution contained (mM): NaCl 148, KCl 5.4, $CaCl_2$ 1.8, $MgCl_2$ 1, HEPES 15, $NaHPO_4$ 0.4, D-glucose 5.5 and pH adjusted to 7.4 (NaOH). Diastolic calcium ratio was analyzed (IonWizard, IonOptix; Origin 6). Each myocyte was paced for 1 minute before recording 10 consecutive CaTs for analysis. Cells from WT and R67Q$^{+/-}$ mice were used and CaTs measured at baseline and following incubation with isoproterenol (10 nmol/L). In a separate set of experiments, calcium tolerant RV myocytes were paced for 30 seconds at 2 Hz then treated with caffeine (10 mmol/L) and SR calcium content and NCX ($Na^+/Ca^{2+}$-exchanger) activity were analyzed.

## Spontaneous Event Quantification

Occurrence of triggered activity of both EADs and DADs observed during AP recordings were quantified using event detection in pClamp 10. Cells were paced at each frequency for 1 minute and each 1-minute period was analyzed, per frequency per cell during pacing for quantification of EADs. Rejection threshold was set at 20 mV for EAD detection, as EADs rarely passed this threshold, thus excluding APs that did pass 20 mV from being included in analyses. DAD quantification occurred

in the 1-minute following cessation of pacing per frequency per cell and were observed as membrane oscillations, and oscillations that reached threshold elicited an AP. Data were analyzed using pClamp 10 and Origin 6 and shown as mean events/cell.

Spontaneous calcium release events during ratiometric CaT measurements were quantified by manually counting increases in 340/380 ratio following cessation of pacing over a 1-minute recording time for each frequency for each cell. Data were analyzed using IonWizard and Origin 6 and shown as mean events/cell.

## Western Blot

Mouse hearts were homogenized under liquid nitrogen to a fine powder and lysed in lysis buffer containing (mM) Tris 50, NaCl 150, Triton X-100 1%, Sodium deoxycholate 0.5% supplemented with 2 mmol/L phenylmethane sulfonyl fluoride and protease inhibitors. Lysates were incubated on ice followed by sonication and insoluble material removed by centrifugation. Approximately 100 µg of whole heart lysates were analyzed by SDS-PAGE and Western blotting.[31] Membranes were incubated with anti-Kir2.1 (Santa Cruz, Dallas, TX), anti-GAPDH (BD Bioscience, San Jose, CA), anti-SERCA2A (ThermoFisher, MA), anti-NCX1 (sodium/calcium exchanger; Swant, Switzerland), and anti-RyR2 (ThermoFisher, MA) then incubated with HRP-conjugated secondary antibodies. Western blots were imaged using a GE Amersham Imager 600. Densitometry data were analyzed using ImageJ and Origin 6.

## Hematoxylin and Eosin Histology

Age- and sex-matched mouse hearts of WT and R67Q$^{+/-}$ were excised and perfused with 4% paraformaldehyde. Hearts were cut in 4-chambered view and embedded in paraffin, then processed for histological analysis at the UW Department of Surgery Histology Core. Five to six micrometers sections of the paraffin-embedded hearts were stained with Hematoxylin and Eosin (H&E). Briefly, dry paraffin slides were deparaffinized and rehydrated by incubating at 60°C for 20 minutes followed by incubation in xylene and then ethanol. Sections were rinsed in water and stained with Harris Hematoxylin and Eosin sequentially, with sections washed with water and ethanol in between each stain. Tissue sections were then dehydrated by rinsing in ethanol and xylene before mounting with cytoseal using coverslips. Images were acquired using an EVOS cell imaging system (ThermoFisher Scientific, MA) with bright field using a 10× objective. Area scanning and tile stitching feature was used to generate the images shown.

## Statistics

All data are presented as mean±SE. Statistical comparisons were carried out using Student unpaired *t*-test (see Table 1, Figure 3B). Two-way repeated measures ANOVA with post hoc Bonferroni correction was used for electrophysiological and CaT analyses (see Table 2, Figures 3C, 4B, 5B through 5F, 6B), or nonlinear regression analysis (see Figure 6C and 6D) using OriginLab (Northampton, MA). Differences were significant at $P<0.05$. Repeated measures for Table 2 were treatment (column factor) and duration (row factor). For duration, $P<0.0001$ and for treatment, $P<0.05$. Multiple comparisons were carried out using Prism 8 by GraphPad, to allow comparison of different APDs and treatments within the same dataset. Bonferroni correction is applied to correct for multiple comparisons.

# RESULTS

## Human Cardiac Phenotype Is Recapitulate by R67Q$^{+/-}$ Mice: Adrenergic-Dependent BiVT and Structurally Normal Hearts

The index patient who presented to the UW Inherited Arrhythmia Clinic at age 33 with symptoms of teen-age onset of exertional syncope and dyspnea.[11] She has a structurally normal heart by echocardiogram, no coronary artery disease, and is heterozygous for the *KCNJ2* R67Q mutation. The patient underwent Holter monitor testing before initiating any medications. Quantification of Holter data revealed that 28% of all QRS complexes were ventricular in origin, no atrial arrhythmia nor atrial ectopy occurred, and there were 1616 runs of PMVT and BiVT. Figure 1A includes one of the Holter recorded ventricular runs that occurred during exercise demonstrating 4 beats of BiVT followed by a sinus complex and then 22 beats of PMVT before the arrhythmia spontaneously terminates. Other Holter recorded runs of PMVT occurred with activity but were shorter and none occurred during sleep.

To study the whole animal and arrhythmia phenotype, WT and R67Q$^{+/-}$ mice underwent echocardiogram, cardiac morphological characterization, and ECG analysis. Echocardiographic comparison at 8 to 12 weeks old (summarized in Table I in the Data Supplement) revealed all parameters including ejection fraction, ventricular size in systole and diastole, and stroke volume were comparable between WT and R67Q$^{+/-}$. Shown in Figure 1B is a H&E stained 4-chamber display of WT and R67Q$^{+/-}$ demonstrating normal myocyte architecture and centrally placed nuclei for both genotypes. Together, these results establish that R67Q$^{+/-}$ mice are not functionally distinct from WT littermates and do not have cardiac structural abnormalities.

WT and R67Q$^{+/-}$ mice ECG recordings were analyzed blinded to genotypes and are summarized in Table 1. Baseline parameters in WT and R67Q$^{+/-}$ mice showed sinus rhythm with normal intervals (Table 1; Figure 1) and without differences between groups. In humans, there is a strong correlation between shorter RR intervals and QT shortening; however, the relationship between QT and RR in mice is weak, and correction formulae, routinely used in human ECG interpretation, have been shown to be misleading.[32,33] Mice received an intraperitoneal injection of caffeine (120 mg/kg) and epinephrine (2 mg/kg) and ECGs recorded for up to 30 minutes. As shown in Table 1, RR interval decreased in WT and R67Q$^{+/-}$ following epinephrine and caffeine ($P<0.05$), but QRS and QT intervals were unaffected ($P>0.05$). After adrenergic

**Table 1. Electrocardiographic Assessment of R67Q$^{+/-}$ Following Epinephrine and Caffeine Administration**

| Parameter | WT Baseline | WT Post Epi and Caffeine | R67Q$^{+/-}$ Baseline | R67Q$^{+/-}$ Post Epi and Caffeine |
|---|---|---|---|---|
| RR, ms | 122.5±5.01 | 95.9±4.4* | 118.5±3.7 | 95.9±3.6† |
| PR, ms | 37.7±0.6 | 43.6±1.8 | 38.9±0.9 | 44.9±2.7 |
| QRS, ms | 15.6±0.5 | 16.4±0.3 | 15.7±0.4 | 17.4±0.8 |
| QT, ms | 39.3±1.02 | 39.0±0.5 | 40.1±0.7 | 39.6±1.1 |

Values are means±SE. Shown is the quantification of electrocardiography parameters in R67Q$^{+/-}$ and WT mice at 8 to 12 wks of age, at baseline and following intraperitoneal injection of epinephrine and caffeine. ECGs were quantified 5-min post-injection of adrenergic stimulus. N=8 per group. Student *t*-test was used to determine significance difference between groups. Epi indicates epinephrine; and WT, wild type.

*$P$<0.001 compared with those at baseline.

†$P$<0.01 compared with those at baseline.

stimulation, R67Q$^{+/-}$ mice developed paroxysms of BiVT, frequent premature ventricular contractions, ventricular bigeminy, and ventricular tachycardia (VT) (Figure 1C, example of BiVT shown in Figure 1D following adrenergic challenge, VT shown in Figure 1E). WT mice showed sinus tachycardia and 26% of WT also had rare, isolated PVCs (example shown in Figure 1E), but none developed BiVT, VT or sustained arrhythmia (Figure 1C). Frequency of arrhythmia types recorded is shown in Figure 1C, and development of arrhythmic phenotype was not dependent upon animal sex (Figure IIA in the Data Supplement).

## Spontaneous Sustained Ventricular Arrhythmia in R67Q$^{+/-}$ Hearts

We performed optical mapping of the anterior ventricular epicardium of R67Q$^{+/-}$ versus WT Langendorff-perfused hearts. Baseline rhythm was sinus and pseudo-ECG (black trace), optical action potential (OAP, blue trace), and activation maps demonstrate reproducible and similar activation patterns between WT (Figure 2A and 2B) and R67Q$^{+/-}$ (Figure 2C and 2E). Figure 2B and Figure 2E are the representative activation map for

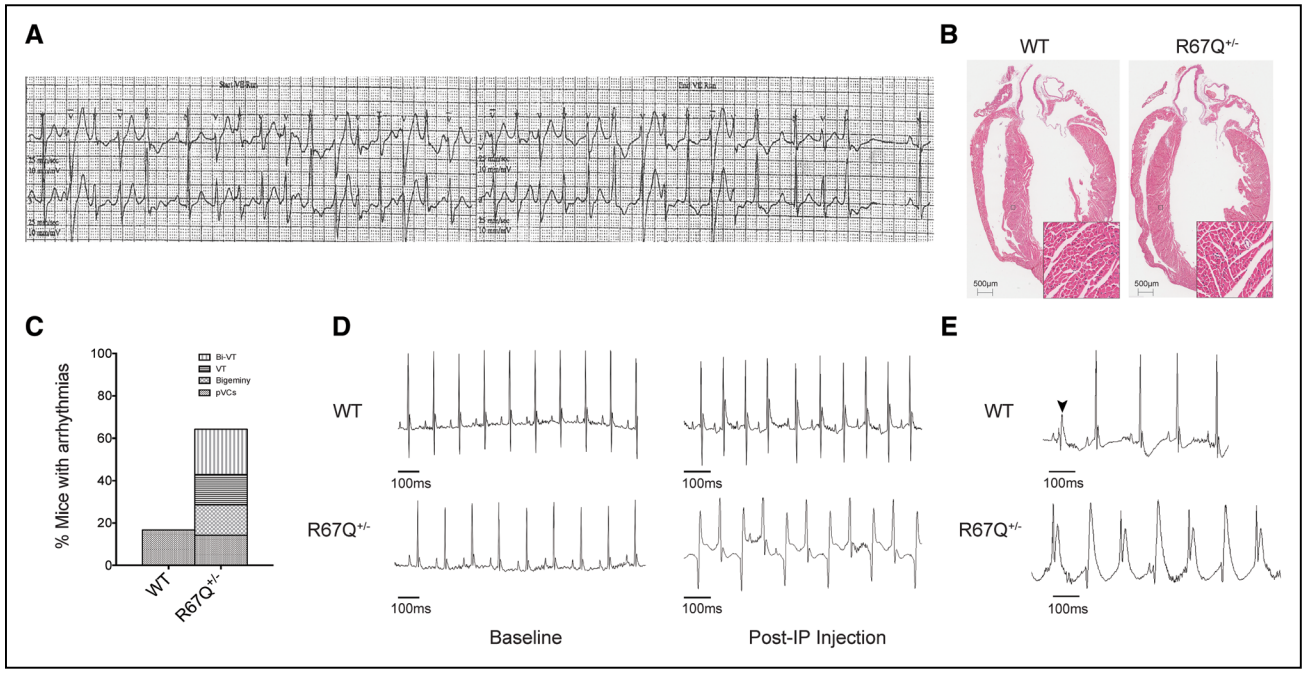


**Figure 1. R67Q$^{+/-}$ mice develop paroxysmal bidirectional ventricular tachycardia (VT) following administration of caffeine and epinephrine.**

**A**, Tracing from a Holter monitor of the patient with R67Q mutation showing bidirectional ventricular tachycardia and polymorphic ventricular tachycardia. **B**, Hematoxylin and Eosin staining of whole heart from wild-type (WT) and R67Q$^{+/-}$. Gross histology revealed no significant difference between WT and R67Q$^{+/-}$ in heart structure and size. Scale bar is 500 µm. Insert scale is 50 µm. **C**, Quantification of arrhythmic events observed in WT and R67Q$^{+/-}$ during ECG analysis. **D**, ECG recorded from anesthetized WT (top) and R67Q$^{+/-}$ (bottom) mice at baseline for 5 min. Normal sinus rhythm was observed in both groups. Epinephrine (2 mg/kg) and caffeine (120 mg/kg) were administered by intraperitoneal injection (IP) injection and ECG recorded for up to 30 min. WT showed faster sinus rhythm (top right), whereas R67Q$^{+/-}$ mice developed paroxysm of bidirectional ventricular tachycardia (bottom right taken at 10-min post-injection). **E**, Upper trace shows a representative premature ventricular contraction (PVC) observed in WT mice following injection of caffeine and epinephrine. PVC is highlighted by the arrow. Lower trace shows representative polymorphic ventricular tachycardia observed in R67Q$^{+/-}$ following injection. N=8 animals per group.

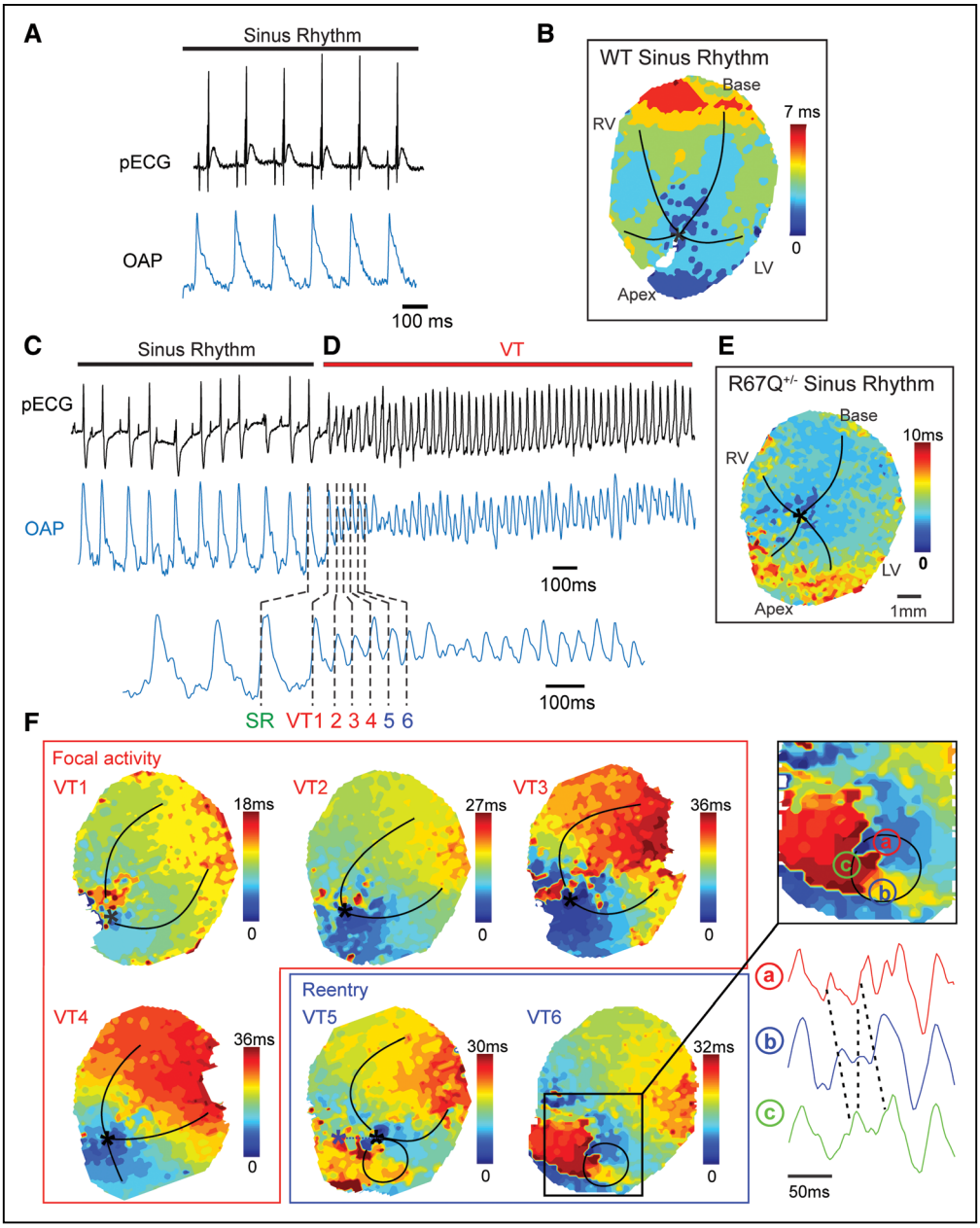


**Figure 2. Epinephrine and caffeine administration results in ventricular arrhythmia in Langendorff-perfused R67Q$^{+/-}$ heart.** **A**, Sinus rhythm pseudo ECG (pECG) from intact wild-type (WT) heart (black trace) and optical action potential (OAP, blue trace). **B**, Activation map for sinus rhythm from intact WT heart. **C**, Sinus rhythm pECG from intact heart (black trace) and optical action potential (OAP, blue trace). **D**, Spontaneous ventricular tachycardia following adrenergic stimulation captured on pECG and OAP. **E**, Activation map for sinus rhythm from intact heart. **F**, Focal activity activation maps from OAP beats VT1-4. Initiation of focal activity is indicated with a black asterisk. Lower right, progression to focal reentry in beats VT5 and VT6. Inset shows reentry activation pattern and OAP delay between a, b and c. N=3/group. LV indicates left ventricle; RV, right ventricle; SR, sinus rhythm; and VT, ventricular tachycardia.

sinus rhythm for WT and R67Q$^{+/-}$, respectively, showing impulse generation exiting from the conduction system normally and spreading throughout the heart. Under basal conditions, there were no spontaneous arrhythmias in either group. Based on previous murine models for VT induction,[34] we treated the excised hearts with caffeine (2.5 mmol/L) plus epinephrine (0.8 μM) with extracellular [$Ca^{2+}$] 1.8 mmol/L. Following treatment, 100% of the R67Q$^{+/-}$ hearts had induction of spontaneous sustained VT within 14 to 19 minutes from the time of caffeine plus epinephrine perfusion. Figure 2C shows an example pseudo-ECG from a R67Q$^{+/-}$ heart in sinus rhythm that transitions to wide complex tachycardia as shown in Figure 2D. Focal activity, as demonstrated by the highlighted individual beats (VT1–VT4) in Figure 2F, initiates PMVT from the ventricular apex region. This then progresses to focal reentry, shown in the activation map (Figure 2F, VT5 and VT6). In contrast, with the same protocol, WT hearts

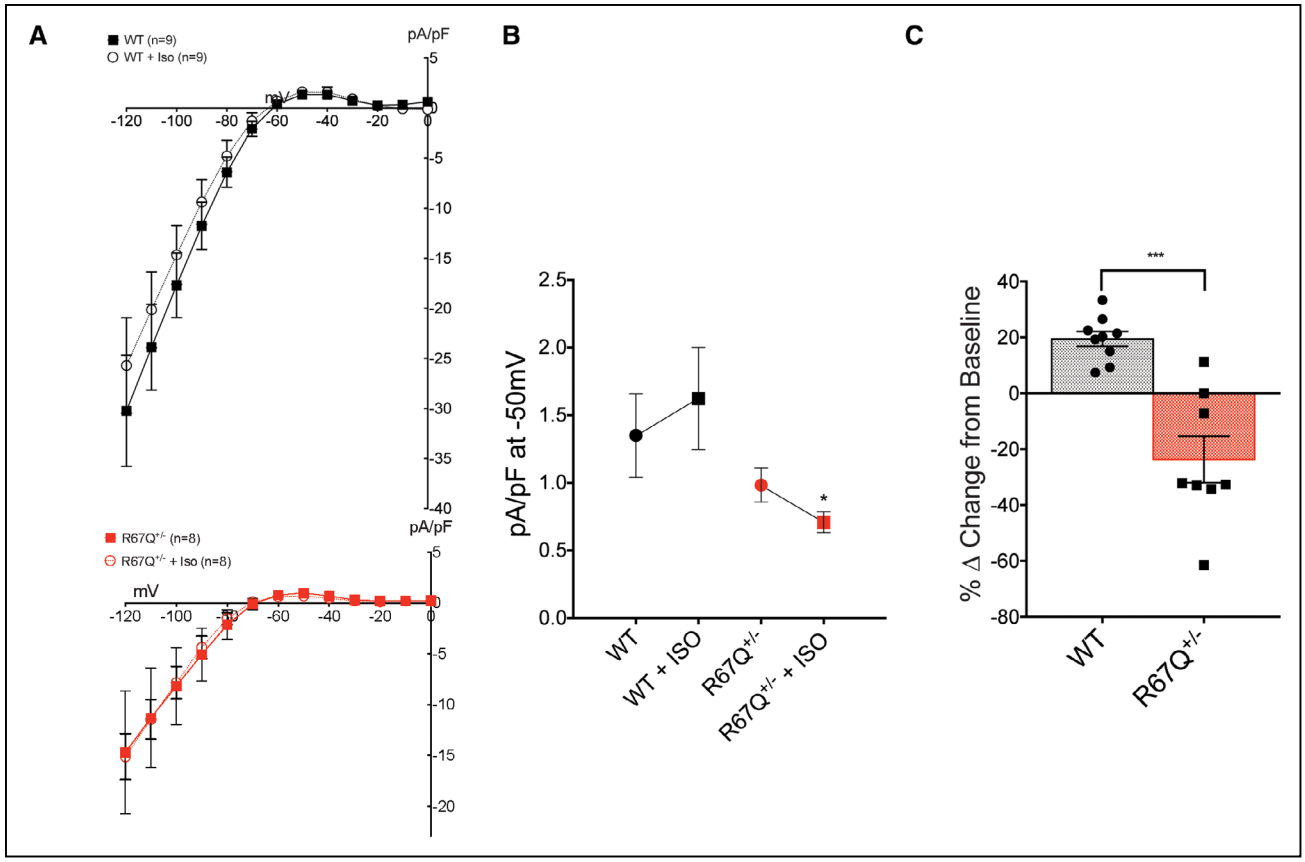


**Figure 3. $I_{K1}$ fails to increase following isoproterenol.**
**A**, Baseline current voltage relationship for wild-type (WT; black squares, N=5, n=9), R67Q$^{+/-}$ (red squares, N=5, n=8). Following isoproterenol (ISO) perfusion for 5 min, WT outward current (black open circles, N=5, n=9) increased; however, R67Q$^{+/-}$ outward current (red open circles, N=5, n=8) decreased in response to adrenergic stress. Currents shown are calculated following barium subtraction. Barium is perfused for 2 min following final ISO measurement. **B**, Absolute current values at −50 mV following ISO treatment: R67Q$^{+/-}$ outward $I_{K1}$ (0.71±0.08 pA/pF) is significantly decreased compared with WT (1.62±0.38 pA/pF) following isoproterenol treatment ($P$<0.05). **C**, Peak outward current was determined at −50 mV, and the percentage change for each cell from baseline was calculated. The delta from baseline showed a 19.5±2.7% increase in outward current at −50 mV in WT cells (black, N=5, n=9), whereas R67Q$^{+/-}$ cells (red, N=5, n=8) showed a 23.7±8.3% decrease in outward current at −50 mV. ***$P$<0.001. Student $t$-test was used to determine significance difference between groups (**B**), or two-way repeated measures ANOVA with post hoc Bonferroni correction was used (**C**).

failed to demonstrate sustained arrhythmia. Nearly 40 minutes after the infusion of caffeine and epinephrine, 1 of 3 WT hearts had spontaneous arrhythmia that lasted only 2 minutes and then spontaneously terminated. Using a low dose of caffeine (1 mmol/L) plus epinephrine (0.8 μM) with either 1.2 to 1.8 mmol/L extracellular [$Ca^{2+}$] did not result in any spontaneous arrhythmias (N=2/group) nor did perfusion of 100 nmol/L isoproterenol (without caffeine or epinephrine; N=2/group).

## Paradoxical Response of R67Q$^{+/-}$ to Adrenergic Stimulation Compared With WT

$I_{K1}$ was measured from isolated cardiomyocytes sequentially at baseline and after 10 nmol/L isoproterenol (representative figures in Figures III and IVA in the Data Supplement). Myocytes isolated from the RV free wall were used as Kir2.1 expression is variable throughout the ventricles, and expression of Kir2.1 is more consistent cell to cell in the right ventricle.[35] WT and R67Q$^{+/-}$ myocytes demonstrated a typical inward-rectifier N-shaped current-voltage (*IV*) relationship with maximal outward current at −50 mV (Figure 3A, rectification index summary data in Figure IVB in the Data Supplement). For comparisons, we focused on the most physiological component of $I_{K1}$, which is the outward current as cardiomyocytes are not polarized below −90 mV. Outward current amplitude at baseline was not significantly different in R67Q$^{+/-}$ cells compared with WT cells, Figure 3B. With isoproterenol infusion, WT myocytes demonstrated an increase at −50 mV in absolute outward current values as well as percent increase from baseline (Figure 3B and 3C). In contrast, R67Q$^{+/-}$ myocytes showed decreased at −50 mV in absolute outward current and percent decreased from baseline ($P$<0.001) (Figure 3B and 3C). Thus, the difference in $I_{K1}$ repolarization drive between R67Q$^{+/-}$ and WT is ≈43%. Absolute current values showed a similar effect at −40 mV with WT $I_{K1}$ increased, whereas R67Q$^{+/-}$ $I_{K1}$

**Table 2. Action Potential Characteristics in WT and R67Q$^{+/-}$ Myocytes at Baseline and Following Isoproterenol**

| Condition | RMP, mV | dV/dT$_{max}$, V/s | APA, mV | APD$_{10}$, ms | APD$_{50}$, ms | APD$_{70}$, ms | APD$_{90}$, ms |
|---|---|---|---|---|---|---|---|
| WT | | | | | | | |
| 2 Hz | −70.91±0.71 | 232.40±15.57 | 117.60±1.88 | 0.37±0.03 | 3.36±0.58 | 7.76±1.22 | 35.97±3.40 |
| 4 Hz | −71.27±1.19 | 244.40±6.13 | 115.40±2.06 | 0.40±0.03 | 3.44±0.64 | 8.31±1.35 | 38.88±3.86 |
| 6 Hz | −71.85±1.55 | 245.00±8.55 | 112.30±2.10 | 0.42±0.04 | 3.79±0.72 | 9.65±1.62 | 40.66±3.44 |
| WT+ISO | | | | | | | |
| 2 Hz | −74.66±0.75* | 256.10±9.51 | 118.20±1.43 | 0.40±0.04 | 4.76±0.77 | 8.94±1.29 | 32.33±2.13 |
| 4 Hz | −76.51±1.13* | 257.90±9.03 | 118.20±1.49 | 0.45±0.04 | 5.81±0.77 | 11.46±1.53 | 39.63±1.61 |
| 6 Hz | −76.49±1.41 | 256.10±10.05 | 115.80±1.51 | 0.45±0.05 | 6.21±0.89 | 13.42±1.97 | 42.61±3.28 |
| R67Q$^{+/-}$ | | | | | | | |
| 2 Hz | −71.10±0.62 | 268.90±6.54 | 120.90±2.30 | 0.54±0.13 | 7.65±3.26 | 18.79±7.50 | 54.34±13.92* |
| 4 Hz | −70.76±0.93 | 268.90±7.32 | 118.50±2.20 | 0.55±0.13 | 7.07±2.61 | 17.87±5.67 | 55.70±10.02* |
| 6 Hz | −70.10±1.34 | 261.50±8.16 | 114.70±2.03 | 0.59±0.16 | 6.69±2.34 | 19.90±5.19 | 67.76±14.12† |
| R67Q$^{+/-}$+ISO | | | | | | | |
| 2 Hz | −73.90±1.29 | 264.60±8.31 | 118.20±2.92 | 0.74±0.30 | 9.94±3.12 | 18.44±5.10 | 59.10±11.76‡ |
| 4 Hz | −74.25±1.13 | 264.00 ±10.59 | 115.90±3.33 | 0.81±0.32 | 10.81±2.91 | 20.89±5.01 | 62.81±10.30† |
| 6 Hz | −72.97±1.06 | 267.00±11.35 | 110.50±4.18 | 0.86±0.33 | 11.15±2.18 | 23.00±3.26 | 64.38±9.38† |

Values are means±SE. RMP, dV/dT$_{max}$, APA, and APD at 2, 4, and 6 Hz at baseline and following isoproterenol. WT−N=4, n=7; WT+ISO−N=4, n=6; R67Q$^{+/-}$±ISO−N=3, n=5. Two-way repeated measures (Treatment [±ISO] or duration of action potential) ANOVA with post hoc Bonferroni correction was used. Significance levels indicated are following Bonferroni correction. APA indicates action potential amplitude; APD, action potential duration; ISO, isoproterenol; RMP, resting membrane potential; and WT, wild-type.

*$P$<0.05 compared with WT.

†$P$<0.001 compared with WT.

‡$P$<0.01 compared with WT.

decreased to ($P$<0.05; Figure V in the Data Supplement). Importantly, densitometry analysis of Kir2.1 protein expression showed no significant difference between mouse groups (Figure VI in the Data Supplement) suggesting that in R67Q$^{+/-}$ mice adrenergic stimulation results in loss of $I_{K1}$ decreasing the repolarization reserve despite normal Kir2.1 protein expression.

## R67Q$^{+/-}$ Mice Show AP Prolongation at Baseline and Following Isoproterenol

Example AP traces for WT and R67Q$^{+/-}$ at baseline and after incubation with isoproterenol are shown in Figure 4. Analysis of AP morphology showed a longer APD$_{90}$ in R67Q$^{+/-}$ myocytes compared with WT at 2, 4, and 6 Hz, both at baseline ($P$<0.05 at 2 and 4 Hz, $P$<0.001 at 6 Hz) and following isoproterenol ($P$<0.01 at 2 Hz, $P$<0.001 at 4 and 6 Hz; Table 2). The dV/dt$_{max}$ did not differ between WT and R67Q$^{+/-}$ myocytes both at baseline and following isoproterenol (Table 2) at any of the frequencies measured. This is indicative of both normal cellular excitability and normal activation of cardiac sodium channels in R67Q$^{+/-}$ myocytes. Resting membrane potential at baseline did not differ between mouse groups; however, following isoproterenol, resting membrane potential hyperpolarized in WT cells ($P$<0.05) at 2 and 4 Hz (normal physiological response), but not in R67Q$^{+/-}$ cells ($P$>0.1), consistent with lack of $I_{K1}$ augmentation with isoproterenol (Table 2).

## R67Q$^{+/-}$ and WT Have Similar Calcium Handling

Calcium-tolerant isolated RV myocytes were loaded with fluo-4 AM and paced at 1 Hz for 30 seconds, 2 Hz for 15 seconds, and 3 Hz for 15 seconds followed by a pulse of 10 mmol/L caffeine, in the presence and absence of isoproterenol. Representative line scans and transients are shown in Figure 5A. CaT amplitude was not significantly different between WT and R67Q$^{+/-}$ myocytes under basal conditions. Both WT and R67Q$^{+/-}$ CaTs increased in amplitude in response to isoproterenol perfusion, at all frequencies measured. Additionally, the 50% decay time was not significantly different between WT and R67Q$^{+/-}$ at baseline or following isoproterenol, suggesting that $Ca^{2+}$ reuptake/extrusion mechanisms are unaffected by the presence of the mutation. The velocity of the transient was comparable between WT and R67Q$^{+/-}$ at baseline and following isoproterenol, Figure 5E. In a separate set of experiments to determine diastolic $Ca^{2+}$, ratiometric imaging of intracellular $Ca^{2+}$ cycling in isolated ventricular myocytes revealed a similar baseline $Ca^{2+}$ ratio in R67Q$^{+/-}$ versus WT (Figure 5F) that was not significantly different following isoproterenol ($P$>0.05).

SR $Ca^{2+}$ content was estimated by the caffeine transient (Figure 5B) and is similar in R67Q$^{+/-}$ versus WT ventricular myocytes. Following isoproterenol, both WT and R67Q$^{+/-}$ SR $Ca^{2+}$ increase to similar levels. Therefore, R67Q$^{+/-}$ myocytes have no significant differences in SR $Ca^{2+}$ load or $Ca^{2+}$ release and removal compared with WT at baseline. Accordingly, Western blot analysis

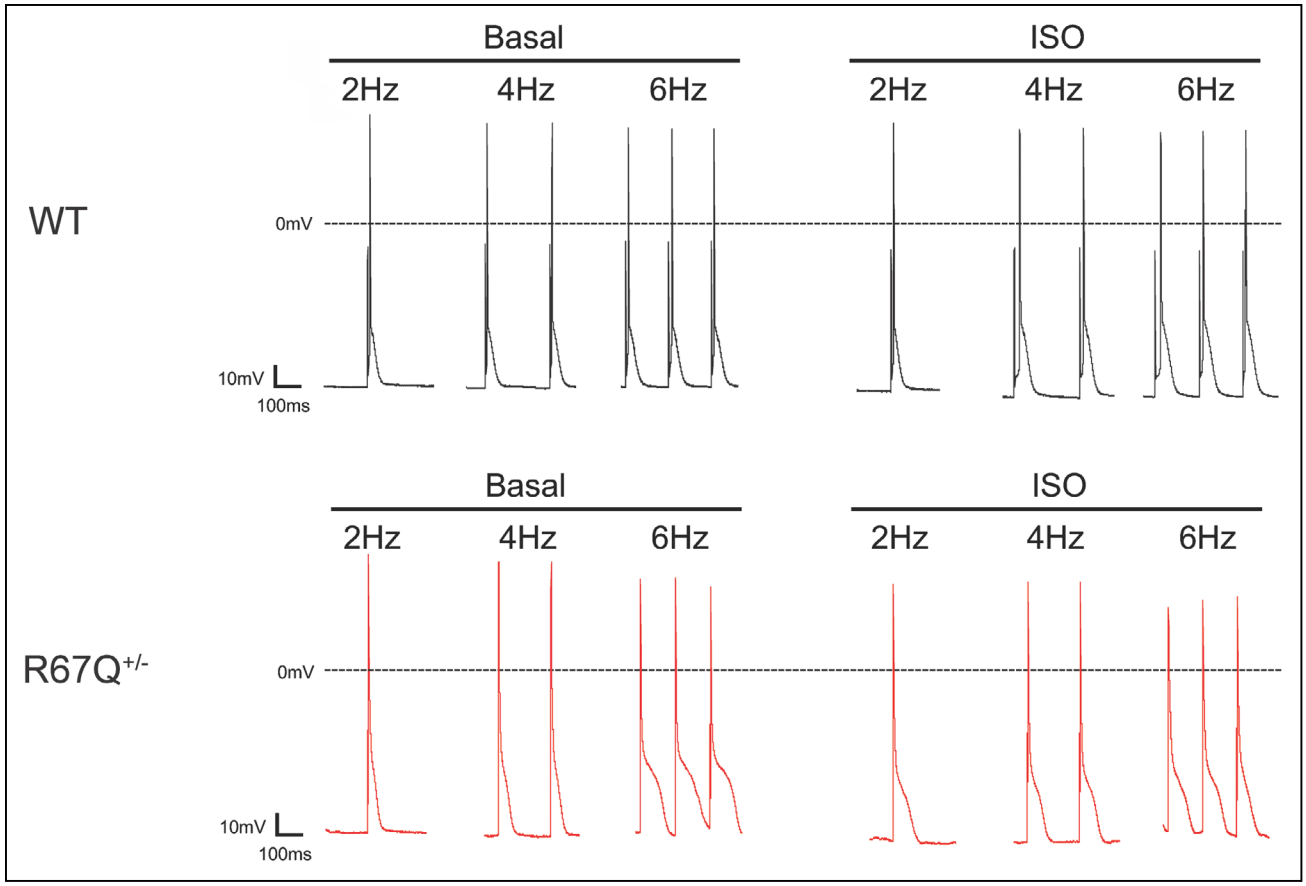


**Figure 4. R67Q$^{+/-}$ myocytes have prolonged APD$_{90}$ (action potential duration at 90%) at baseline and following adrenergic stress.** **A**, Representative action potentials from wild-type (WT; left, upper), WT+isoproterenol (ISO; right, upper), R67Q$^{+/-}$ (left, lower), and R67Q$^{+/-}$+ISO (right, lower) at 2, 4, and 6 Hz. Scale bar represents 100 ms and 10 mV.

from lysates of WT or R67Q$^{+/-}$ mouse hearts did not show any difference in the expression of primary $Ca^{2+}$ handling proteins, RyR2, NCX1, and SERCA2a, between groups (Figure VII in the Data Supplement).

## Adrenergic Stimulation Causes Phase 3 EADs in R67Q$^{+/-}$ Myocytes

An increase in the number of triggered APs during current clamp experiments and spontaneous $Ca^{2+}$ release events during CaT measurements was observed in cells from R67Q$^{+/-}$ mice following isoproterenol compared with WT (Figure 6A at 4 Hz pacing and Figure VIII in the Data Supplement for 6 Hz pacing). In current clamp experiments, R67Q$^{+/-}$ cells had a dramatic increase in the frequency of EADs following isoproterenol while WT had no EADs at baseline and few EADs following isoproterenol. At baseline, R67Q$^{+/-}$ cells had a similar number of DADs as WT cells. A slight increase in DADs was observed in R67Q$^{+/-}$ cells following isoproterenol but did not reach significance ($P$>0.05). Figure 6B is a summary of the number and type of triggered activity events per cell during AP measurements (left panel). Analysis of the EADs are summarized in Figure 6C and 6D. Figure 6C plots the AP voltage that the EAD take-off potential occurs versus the time from the pacing stimulus. Notably, EADs were observed to have a take-off potential at −38 to −52 mV along with rapid re-activation. Regression analysis of the EAD take-off potential versus peak voltage is plotted in Figure 6D. Integrating the stimulation of EADs by isoproterenol, their take-off potential voltage, and morphological characteristics with steep reactivation are consistent with other reports of phase 3 EADs.[36–38] Unlike phase 2 EADs, the AP is not exceedingly prolonged and some reports of phase 3 EADs not an AP shortening.[38] The take-off potential is below $I_{CaL}$ window activation range and accordingly may depend on $I_{Na}$ at least as the initial inward charge driver.[38] These are in contrast to phase 2 EADs with a less negative take-off potential and depend on window $I_{CaL}$ activation for the inward charge.[39,40]

Spontaneous $Ca^{2+}$ release events were noted after rapid pacing and isoproterenol infusion for the R67Q$^{+/-}$ during CaT measurements but not WT. These delayed $Ca^{2+}$ release events, shown in example traces in Figure 6A, right, could be consistent with DADs.[39,41] Figure 6B right panel quantifies the spontaneous $Ca^{2+}$ releases during $Ca^{2+}$ transient measurements. WT cells showed comparable spontaneous release events at baseline and following

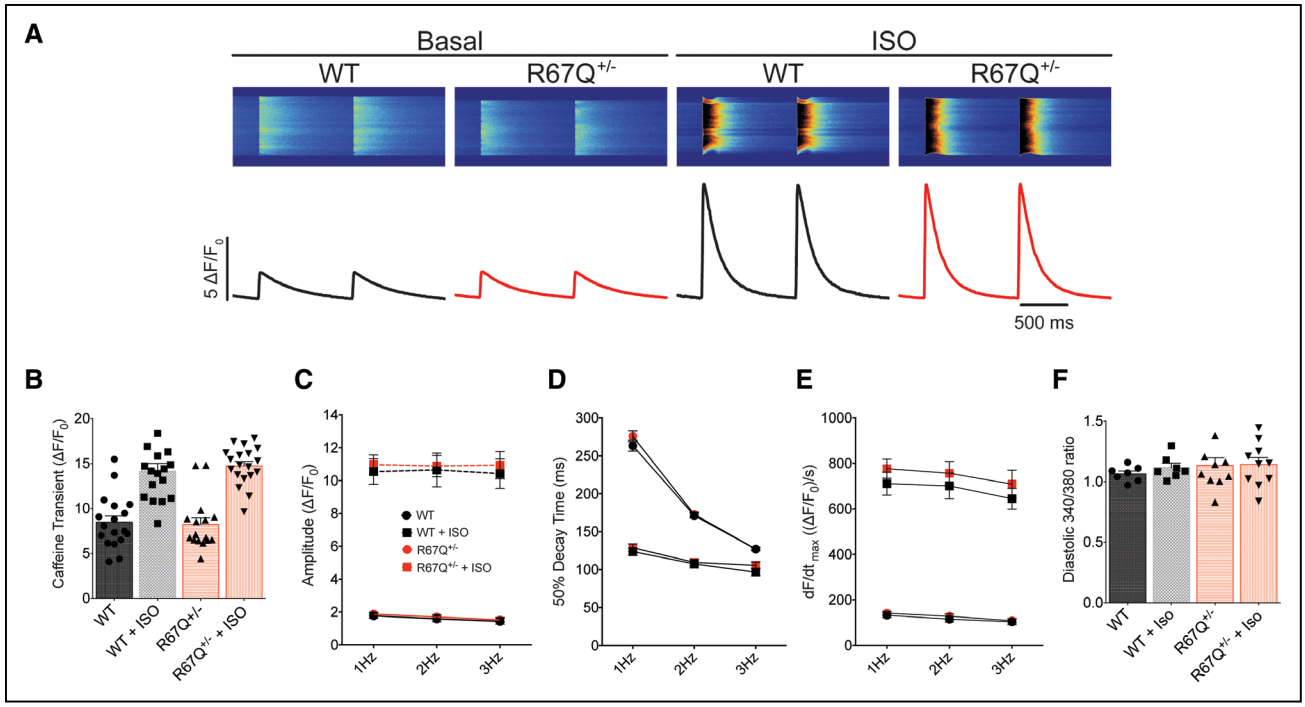


**Figure 5. R67Q$^{+/-}$ does not impact Ca$^{2+}$ handling.**
**A**, Representative calcium transient line-scans from wild-type (WT) and R67Q$^{+/-}$ myocytes. Cells were paced for 30 s at 1 Hz, 15 s at 2 Hz, and 15 s at 3 Hz, followed by a pulse of 10 mmol/L caffeine to measure sarcoplasmic reticulum (SR) content. **B**, WT and R67Q$^{+/-}$ myocytes had comparable SR calcium loads at baseline (8.48±0.70 $\Delta F/F_0$ vs 8.23±0.73 $\Delta F/F_0$, respectively, $P>0.1$) and following treatment with isoproterenol (ISO; 14.17±0.84 $\Delta F/F_0$ vs 14.75±0.49 $\Delta F/F_0$; WT–N=4, n=18; R67Q$^{+/-}$–N=4, n=16). **C**, No significant difference was observed in calcium transient amplitude between WT (black circles) and R67Q$^{+/-}$ (red circles) at baseline or following ISO (WT, black squares, R67Q$^{+/-}$, red squares; WT–N=4, n=18; R67Q$^{+/-}$–N=4, n=16). **D**, Fifty percentage decay time was not significantly different between WT and R67Q$^{+/-}$ at baseline or following ISO (WT–N=4, n=18; R67Q$^{+/-}$–N=4, n=16). **E**, Velocity of the transient ($dF/dt_{max}$) is not significantly different between WT and R67Q$^{+/-}$ at baseline or following ISO (WT–N=4, n=18; R67Q$^{+/-}$–N=4, n=16). **F**, Ratiometric calcium transient measurements show no significant difference in diastolic calcium between WT and R67Q$^{+/-}$ ventricular myocytes ($P>0.05$; WT–N=6, n=7; R67Q$^{+/-}$–N=4, n=10). Two-way repeated measures ANOVA with post hoc Bonferroni correction was used (**B**–**F**).

isoproterenol. At baseline, R67Q$^{+/-}$ cells had comparable events to WT cells. Following isoproterenol, R67Q$^{+/-}$ cells had significantly more events compared with WT cells (see Figure IX in the Data Supplement for data at 6 Hz pacing). These data parallel the arrhythmia susceptibility demonstrated in R67Q$^{+/-}$ ECG recordings with a dramatic increase in events following adrenergic stimulation similar to the patient harboring R67Q mutation.

## Arrhythmia Mechanism

Our collection of in vivo data and analysis in the first transgenic patient-inspired *KCNJ2* mutation mouse model points to a cascade of events leading to triggered activity and arrhythmia in R67Q$^{+/-}$ mice. Unifying our observations, we propose a mechanistic concept that is depicted in the graphical abstract. Adrenergic loss of $I_{K1}$ causes a critical change in membrane voltage that decreases repolarization reserve and drives the development of phase 3 EADs. Our findings are consistent with other models of phase 3 EAD initiation under conditions of decreased repolarization reserve and low extracellular potassium reducing $I_{K1}$[22] and have been mechanistically theorized by other groups.[42] Initially, we anticipated that because the clinical phenotype mimics CPVT, the arrhythmia mechanism would be DAD dependent[43] and that EADs would not be present because of lack of patient and mouse QT prolongation,[39] despite that *KCNJ2* loss of function mutations were initially categorized as long QT syndrome.[10] In contrast to our model, QT prolongation and a tendency for phase 2 EADs are described in other long QT syndrome murine models for which the action potential duration of ventricular myocytes can be twice that of the WT controls[44,45] and EAD take-off potential and morphology is congruent with phase 2 EADs. Instead, our data support adrenergic-dependent phase 3 EADs, which are thought to arise from a combination of EADs and DADs mechanistic events.[44] We propose that understanding the differences in these arrhythmia triggering events, heretofore unknown, will help inform the approach for treatment and arrhythmia suppression strategy.

# DISCUSSION

This is the first patient-inspired *KCNJ2* mutation in vivo model, and we show that R67Q$^{+/-}$ mice mimic the

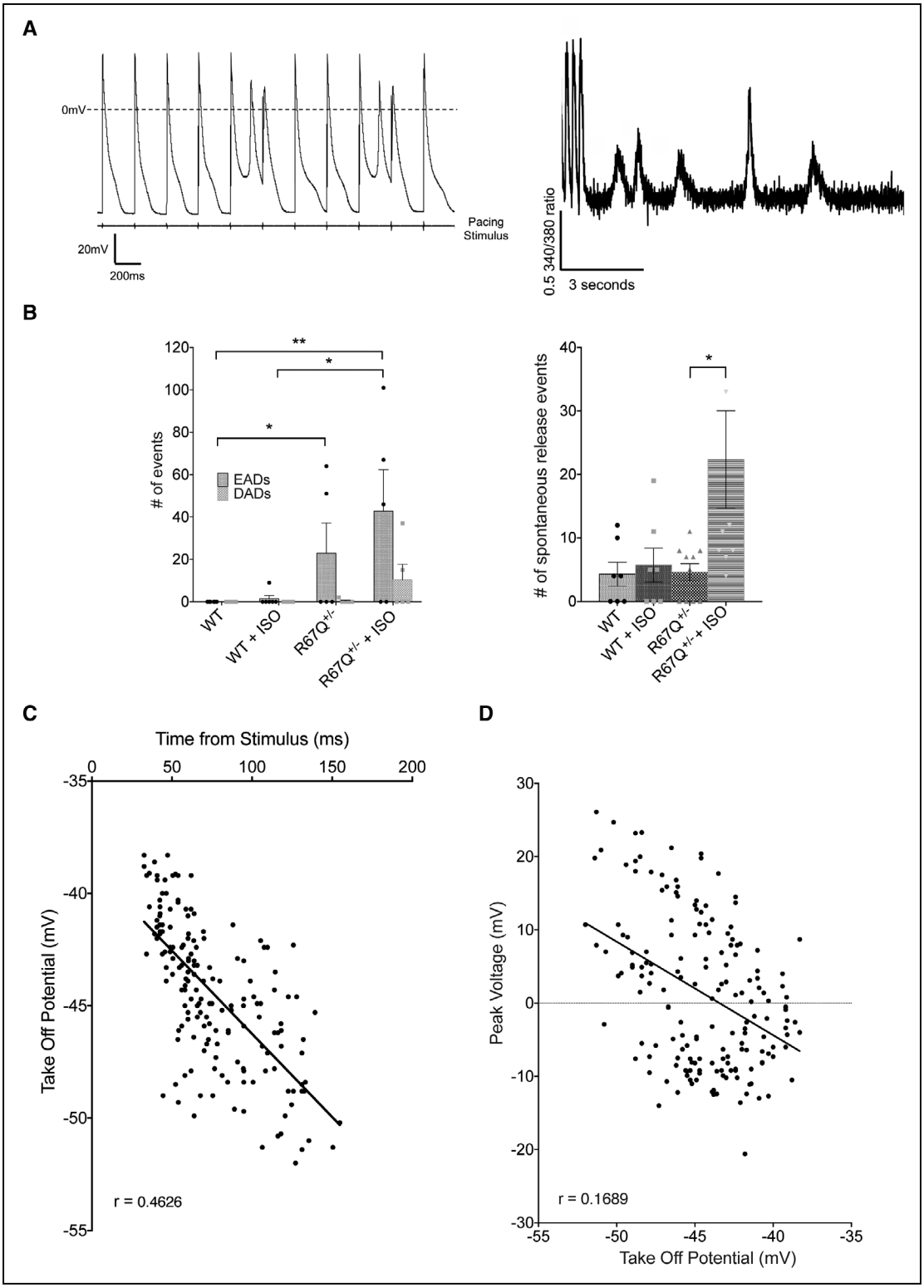


**Figure 6. Adrenergic-dependent phase 3 early afterdepolarizations (EADs) and spontaneous $Ca^{2+}$ oscillations in R67Q$^{+/-}$ mice.** **A**, Representative traces from action potential recordings (left) and calcium transient measurements (right) showing phase 3 EADs and spontaneous $Ca^{2+}$ release events, respectively, from isolated R67Q$^{+/-}$ ventricular myocytes. **B**, R67Q$^{+/-}$ myocytes had more EADs at baseline (23±14.2 events) and following isoproterenol (ISO; 42.8±19.6 events) compared with wild-type (WT; 0 events at baseline, 1.5±1.5 events following ISO; left) during action potential measurements and increased spontaneous release events following ISO during calcium transient measurements (right). **C**, Analysis of take off potential revealed depolarized potential compared with classical phase 2 EADs, with delayed onset from stimulus. **D**, Linear regression of take off potential vs peak voltage reached by phase 3 EADs in R67Q$^{+/-}$ myocytes (animals/cells for EAD analysis: WT–N=3, n=7; R67Q$^{+/-}$–N=2, n=5. Animals/cells for spontaneous event analysis: WT–N=6, n=7; R67Q$^{+/-}$–N=4, n=10). Two-way repeated measures ANOVA with post hoc Bonferroni correction was used (**B**), or nonlinear regression (**C** and **D**). DAD indicates delayed afterdepolarization.

patient phenotype with adrenergic-induced BiVT with a structurally normal heart. Our data determine that R67Q$^{+/-}$ mice have adrenergic-induced $I_{K1}$ loss causing decreased repolarization reserve, AP prolongation that together cause phase 3 EADs and the arrhythmogenic milieu for BiVT.

## Adrenergic Loss of Function

The critical component of arrhythmogenic vulnerability in the R67Q$^{+/-}$ model lies in the adrenergic loss of $I_{K1}$. We have shown that WT Kir2.1 outward (physiological component) current is augmented following adrenergic stimulation and that some *KCNJ2* mutations result in either a blunted response or a decrease in outward component of $I_{K1}$ in heterologous expression systems.[11,45] In this in vivo model of a *KCNJ2* mutation, we demonstrate that adrenergic challenge causes dynamic of loss of function, causing a 40% decrease in repolarization reserve when compared with WT. The underlying molecular mechanism for R67Q-Kir2.1 adrenergic loss of function is not clear at present but could involve PKA channel phosphorylation disruption and/or an increase in sensitivity to the direct inhibitory effect of divalent cation (calcium) on Kir2.1 channels.[11,46] Kir2.1 channels have at least one known amino acid residue that is phosphorylated by adrenergic activated-PKA. Mutation of the known PKA site, abrogates the effect of adrenergic stimulation on channel function[11,45]; however, R67Q mutation is physically distant from this PKA site. Alternatively, there may be several PKA targets, yet to be identified, that R67Q interacts with directly or the effect may be related to 3-dimensional tetrameric subunit interaction. This and alternative explanations are areas of active investigation in our laboratory.

## Triggered Activity and Phase 3 EAD Generation

EADs are secondary membrane voltage depolarizations that occur during AP repolarization as opposed to DADs, which occur after repolarization. EADs that occur during the plateau phase are phase 2 EADs and prolonged repolarization and bradycardia creates vulnerable conditions for phase 2 EADs because of a longer window for reactivation of L-type $Ca^{2+}$ channels.[39] L-type $Ca^{2+}$ channels' time and voltage dependence require phase 2 EADs to occur after a pause or with bradycardia, and phase 2 EADs are suppressed with faster heart rates. In contrast, phase 3 EADs are less well mechanistically understood but may represent a hybrid of DADs and EADs since some DAD conditions are linked to phase 3 EAD initiation.[47] It has been proposed that phase 3 EADs result from a combination of adrenergic stimulation and SR $Ca^{2+}$ release leading to subsequent $I_{Ti}$ generation (from NCX) causing sodium channel reactivation with a lesser role from L-type $Ca^{2+}$ channels.[48] A defining feature of phase 3 EADs is the negative take-off potential under −35 mV and rapid activation. These features are unique from phase 2 EADs and implicate nonequilibrium reactivation of $I_{Na}$ (window current between −60 and −30 mV) rather than $I_{CaL}$ (window current peaks at −15 mV and spans between −30 and 0 mV)[40] as the initial inward current for phase 3 EADs.

As a strong rectifier, $I_{K1}$ is negligible at AP plateau voltages and therefore loss of $I_{K1}$ is unlikely to induce phase 2 EADs. However, decreased $I_{K1}$ will affect phase 3 of repolarization, and it has been theorized that this will promote EADs at negative voltages spanning the $I_{Na}$ window current.[42] In murine models, EADs have been described with characteristics of both phase 2 EADs[49–51] and those with characteristics of phase 3 EADs, the latter with more negative take-off potential below $I_{CaL}$ activation range and activated by adrenergic stimulation. In our experiments, we predominately note adrenergic dependent triggered activity only in the R67Q$^{+/-}$ mice during AP repolarization with a take-off potential ≈46 mV. Thus, the prevailing triggered activity in our model seems to be in the form of phase 3 EADs and fit with the aforementioned theory of loss of $I_{K1}$ by Qu et al.[42] Again, to contextualize our findings with other studies, loss of $I_{K1}$ during $Ca^{2+}$ loading can cause DAD-driven arrhythmias because of $Ca^{2+}_i/V_m$ coupling gain.[52] This is important with respect to arrhythmogenesis since BiVT is an arrhythmia associated with $Ca^{2+}$ overload and DAD activity.[53] It is logical, then, that a hybrid of EAD and DAD conditions necessary for phase 3 EADs are present in the R67Q$^{+/-}$ mice who demonstrate BiVT under conditions of: (1) adrenergic stimulation, (2) $Ca^{2+}$ loading (rapid pacing or adrenergic stimulation), (3) adrenergic dependent loss of $I_{K1}$, and (4) $AP_{90}$ prolongation.

## Arrhythmia Mechanism

The dominant question we attempted to address with this project was why our patient, heterozygous for *KCNJ2* mutation R67Q,[14] as well as the R67Q$^{+/-}$ mouse do not have arrhythmia at baseline but PMVT and BiVT under adrenergic stress. This is in contrast to patients with Anderson-Tawil Syndrome who do not require adrenergic stimulation for arrhythmia induction. The added layer of adrenergic stimulation as requisite for arrhythmia induction clinically suggests a CPVT-like phenotype and cellular $Ca^{2+}$ mishandling. In our case, adrenergic stimulation did not result in $Ca^{2+}$ mishandling but instead potentiated a loss of $I_{K1}$ repolarization capacity. The adrenergic loss of $I_{K1}$, caused critical changes in the membrane potential to drive phase 3 EAD triggered activity and is congruent with both the patient and mouse arrhythmic activity. This is also congruent with other investigators' hypothesis that an arrhythmia mechanism for $I_{K1}$ loss is phase 3 EADs.[42] In contrast to CPVT-associated arrhythmia mechanisms, the primary arrhythmogenic substrate from our in vivo

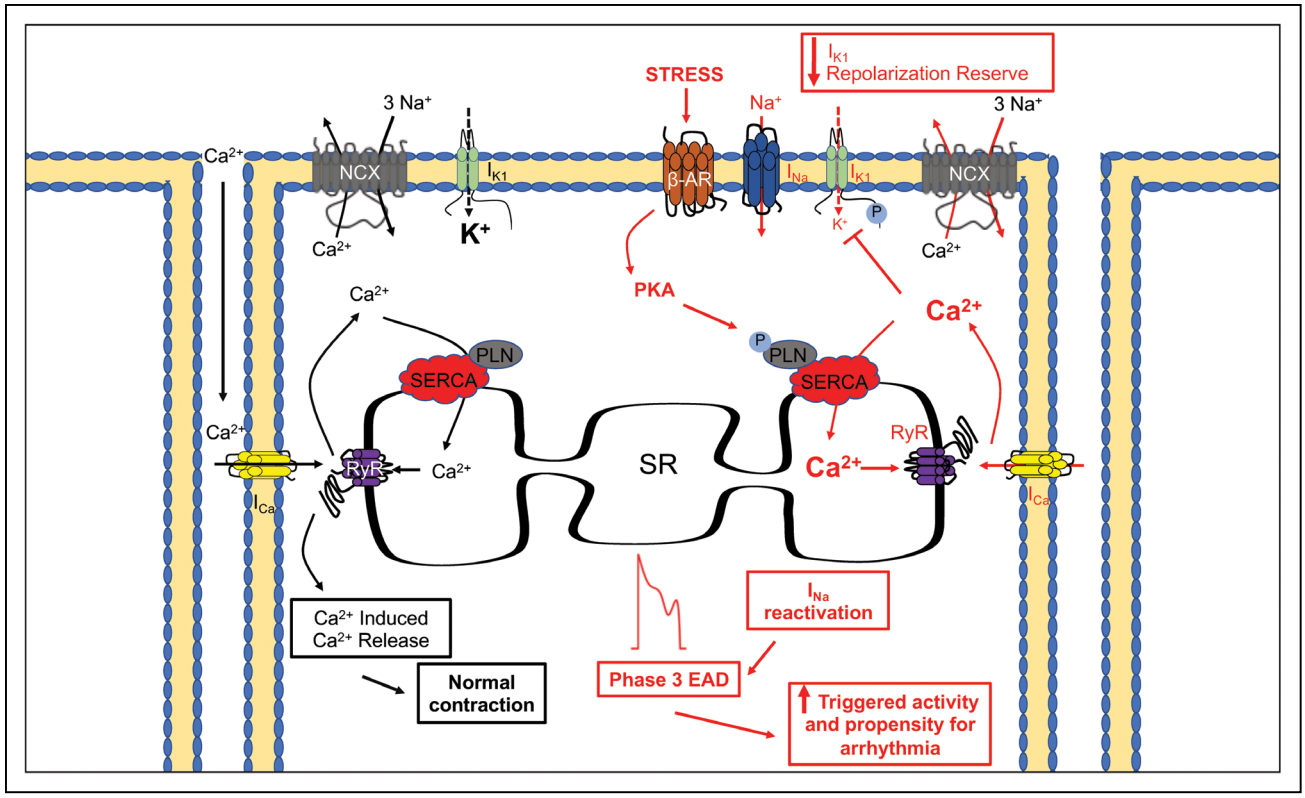


**Figure 7. Proposed arrhythmia mechanism for *KCNJ2* mutation: adrenergic loss of $I_{K1}$ causes a critical change in membrane voltage that decreases repolarization reserve and drives the development of phase 3 early afterdepolarization (EAD).**
PKA indicates protein kinase A; PLN, phospholamban; SERCA, sarcoplasmic reticulum $Ca^{2+}$-ATPase; and SR sarcoplasmic reticulum.

model is the change in membrane voltage because of adrenergic-dependent loss of $I_{K1}$, resulting lack of repolarizing current of the terminal AP leading to phase 3 EAD triggered activity (see cartoon in Figure 7).

## Study Limitations

The whole animal phenotype recapitulates many of the clinical characteristics observed in patients harboring *KCNJ2* mutation. We recognize the limitations and challenges associated with generation of an in vivo model, the differences between human and murine models and translating findings to human clinical phenotypes. However, using in vivo models is necessary to bridge the gaps between mutation to molecular characterization to cellular phenotype and to arrhythmia mechanisms in the whole organ.

# CONCLUSIONS

R67Q$^{+/-}$ mice demonstrate BiVT associated with $I_{K1}$ loss causing decreased-repolarization reserve and resulting in arrhythmogenic phase 3 EADs. These findings advance our understanding of arrhythmia syndromes related to *KCNJ2* mutations and further study of this model will allow us to elucidate more precise treatment approaches based on this arrhythmia mechanism.

## ARTICLE INFORMATION

Received April 1, 2020; accepted June 23, 2020.

### Affiliation

Cellular and Molecular Arrhythmia Research Program, Division of Cardiovascular Medicine, Department of Medicine, University of Wisconsin-Madison.

### Acknowledgments

We thank the technical services provided by the University of Wisconsin-Madison Genome Editing and Animal Models (GEAM) Core and Cardiovascular Resource Core at University of Wisconsin-Madison for technical assistance. We thank Dr Ravi Vaidyanathan for genotyping assistance and Martin Lea for technical advice for myocyte isolation. We thank the members of the Cellular and Molecular Arrhythmia Research Program for constructive discussion. We thank Dr Elenora Grandi for insightful discussion.

### Sources of Funding

This work was supported by National Institutes of Health (NIH R01 HL139738-01 and R01 HL128598-01 to Dr Eckhardt, PPG PO1 HL094291 to Dr Makielski); and the American Heart Association (17POST33670358 to Dr Reilly, 19CDA34660208 to Dr Alvarado).

### Disclosures

None.

## REFERENCES

1. Lopatin AN, Nichols CG. Inward rectifiers in the heart: an update on I(K1). *J Mol Cell Cardiol.* 2001;33:625–638. doi: 10.1006/jmcc.2001.1344
2. Willis BC, Pandit SV, Ponce-Balbuena D, Zarzoso M, Guerrero-Serna G, Limbu B, Deo M, Camors E, Ramirez RJ, Mironov S, et al. Constitutive intracellular Na+ excess in purkinje cells promotes arrhythmogenesis at lower levels of stress than ventricular myocytes from mice with catecholaminergic

polymorphic ventricular tachycardia. *Circulation*. 2016;133:2348–2359. doi: 10.1161/CIRCULATIONAHA.116.021936
3. Donaldson M, Yoon G, Fu Y-H, Ptacek L. Andersen-Tawil syndrome: a model of clinical variability, pleiotropy, and genetic heterogeneity. *Ann Med*. 2009;36:92–97. doi: 10.1080/17431380410032490
4. Priori SG. A Novel Form of Short QT Syndrome (SQT3) is caused by a mutation in the KCNJ2 gene. *Circ Res*. 2005;96:800–807. doi: 10.1161/01.res.0000162101.76263.8c
5. Xia M, Jin Q, Bendahhou S, He Y, Larroque MM, Chen Y, Zhou Q, Yang Y, Liu Y, Liu B, et al. A Kir2.1 gain-of-function mutation underlies familial atrial fibrillation. *Biochem Biophys Res Commun*. 2005;332:1012–1019. doi: 10.1016/j.bbrc.2005.05.054
6. Tester DJ, Arya P, Will M, Haglund CM, Farley AL, Makielski JC, Ackerman MJ. Genotypic heterogeneity and phenotypic mimicry among unrelated patients referred for catecholaminergic polymorphic ventricular tachycardia genetic testing. *Heart Rhythm*. 2006;3:800–805. doi: 10.1016/j.hrthm.2006.03.025
7. Hattori T, Makiyama T, Akao M, Ehara E, Ohno S, Iguchi M, Nishio Y, Sasaki K, Itoh H, Yokode M, et al. A novel gain-of-function KCNJ2 mutation associated with short-QT syndrome impairs inward rectification of Kir2.1 currents. *Cardiovasc Res*. 2012;93:666–673. doi: 10.1093/cvr/cvr329
8. Maruyama M, Lin SF, Chen PS. Alternans of diastolic intracellular calcium elevation as the mechanism of bidirectional ventricular tachycardia in a rabbit model of Andersen-Tawil syndrome. *Heart Rhythm*. 2012;9:626–627. doi: 10.1016/j.hrthm.2010.12.021
9. Morita H, Zipes DP, Morita ST, Wu J. Mechanism of U wave and polymorphic ventricular tachycardia in a canine tissue model of Andersen-Tawil syndrome. *Cardiovasc Res*. 2007;75:510–518. doi: 10.1016/j.cardiores.2007.04.028
10. Eckhardt LL, Farley AL, Rodriguez E, Ruwaldt K, Hammill D, Tester DJ, Ackerman MJ, Makielski JC. KCNJ2 mutations in arrhythmia patients referred for LQT testing: a mutation T305A with novel effect on rectification properties. *Heart Rhythm*. 2007;4:323–329. doi: 10.1016/j.hrthm.2006.10.025
11. Kalscheur MM, Vaidyanathan R, Orland KM, Abozeid S, Fabry N, Maginot KR, January CT, Makielski JC, Eckhardt LL. KCNJ2 mutation causes an adrenergic-dependent rectification abnormality with calcium sensitivity and ventricular arrhythmia. *Heart Rhythm*. 2014;11:885–894. doi: 10.1016/j.hrthm.2014.02.015
12. Leenhardt A, Lucet V, Denjoy I, Grau F, Ngoc DD, Coumel P. Catecholaminergic polymorphic ventricular tachycardia in children. A 7-year follow-up of 21 patients. *Circulation*. 1995;91:1512–1519. doi: 10.1161/01.cir.91.5.1512
13. Priori SG, Napolitano C, Tiso N, Memmi M, Vignati G, Bloise R, Sorrentino V, Danieli GA. Mutations in the cardiac ryanodine receptor gene (hRyR2) underlie catecholaminergic polymorphic ventricular tachycardia. *Circulation*. 2001;103:196–200. doi: 10.1161/01.cir.103.2.196
14. Lahat H, Pras E, Olender T, Avidan N, Ben-Asher E, Man O, Levy-Nissenbaum E, Khoury A, Lorber A, Goldman B, et al. A missense mutation in a highly conserved region of CASQ2 is associated with autosomal recessive catecholamine-induced polymorphic ventricular tachycardia in Bedouin families from Israel. *Am J Hum Genet*. 2001;69:1378–1384. doi: 10.1086/324565
15. Nyegaard M, Overgaard MT, Søndergaard MT, Vranas M, Behr ER, Hildebrandt LL, Lund J, Hedley PL, Camm AJ, Wettrell G, et al. Mutations in calmodulin cause ventricular tachycardia and sudden cardiac death. *Am J Hum Genet*. 2012;91:703–712. doi: 10.1016/j.ajhg.2012.08.015
16. Postma AV, Denjoy I, Hoorntje TM, Lupoglazoff JM, Da Costa A, Sebillon P, Mannens MM, Wilde AA, Guicheney P. Absence of calsequestrin 2 causes severe forms of catecholaminergic polymorphic ventricular tachycardia. *Circ Res*. 2002;91:e21–e26. doi: 10.1161/01.res.0000038886.18992.6b
17. Rooryck C, Kyndt F, Bozon D, Roux-Buisson N, Sacher F, Probst V, Thambo JB. New family with catecholaminergic polymorphic ventricular tachycardia linked to the triadin gene. *J Cardiovasc Electrophysiol*. 2015;26:1146–1150. doi: 10.1111/jce.12763
18. Mohler PJ, Splawski I, Napolitano C, Bottelli G, Sharpe L, Timothy K, Priori SG, Keating MT, Bennett V. A cardiac arrhythmia syndrome caused by loss of ankyrin-B function. *Proc Natl Acad Sci U S A*. 2004;101:9137–9142. doi: 10.1073/pnas.0402546101
19. Barajas-Martinez H, Hu D, Ontiveros G, Caceres G, Desai M, Burashnikov E, Scaglione J, Antzelevitch C. Biophysical and molecular characterization of a novel de novo KCNJ2 mutation associated with Andersen-Tawil syndrome and catecholaminergic polymorphic ventricular tachycardia mimicry. *Circ Cardiovasc Genet*. 2011;4:51–57. doi: 10.1161/CIRCGENETICS.110.957696
20. Kimura H, Zhou J, Kawamura M, Itoh H, Mizusawa Y, Ding WG, Wu J, Ohno S, Makiyama T, Miyamoto A, et al. Phenotype variability in patients carrying KCNJ2 mutations. *Circ Cardiovasc Genet*. 2012;5:344–353. doi: 10.1161/CIRCGENETICS.111.962316
21. Myles RC, Wang L, Bers DM, Ripplinger CM. Decreased inward rectifying K +current and increased ryanodine receptor sensitivity synergistically contribute to sustained focal arrhythmia in the intact rabbit heart. *J Physiology*. 2014;593:1479 1493. doi: 10.1113/jphysiol.2014.279638
22. Maruyama M, Lin SF, Xie Y, Chua SK, Joung B, Han S, Shinohara T, Shen MJ, Qu Z, Weiss JN, et al. Genesis of phase 3 early afterdepolarizations and triggered activity in acquired long-QT syndrome. *Circ Arrhythm Electrophysiol*. 2011;4:103–111. doi: 10.1161/CIRCEP.110.959064
23. Priori SG, Wilde AA, Horie M, Cho Y, Behr ER, Berul C, Blom N, Brugada J, Chiang CE, Huikuri H, et al. HRS/EHRA/APHRS expert consensus statement on the diagnosis and management of patients with inherited primary arrhythmia syndromes: document endorsed by HRS, EHRA, and APHRS in May 2013 and by ACCF, AHA, PACES, and AEPC in June 2013. *Heart Rhythm*. 2013;10:1932–1963. doi: 10.1016/j.hrthm.2013.05.014
24. Nagy A, Rossant J, Nagy R, Abramow-Newerly W, Roder JC. Derivation of completely cell culture-derived mice from early-passage embryonic stem cells. *Proc Natl Acad Sci U S A*. 1993;90:8424–8428. doi: 10.1073/pnas.90.18.8424
25. Zaritsky JJ, Eckman DM, Wellman GC, Nelson MT, Schwarz TL. Targeted disruption of Kir2.1 and Kir2.2 genes reveals the essential role of the inwardly rectifying K(+) current in K(+)-mediated vasodilation. *Circ Res*. 2000;87:160–166. doi: 10.1161/01.res.87.2.160
26. Liu P, Jenkins NA, Copeland NG. A highly efficient recombineering-based method for generating conditional knockout mutations. *Genome Res*. 2003;13:476–484. doi: 10.1101/gr.749203
27. Brody MJ, Feng L, Grimes AC, Hacker TA, Olson TM, Kamp TJ, Balijepalli RC, Lee Y. LRRC10 is required to maintain cardiac function in response to pressure overload. *Am J Physiol Heart Circ Physiol*. 2016;310:H269–H278. doi: 10.1152/ajpheart.00717.2014
28. Salama G, London B. Mouse models of long QT syndrome. *J Physiol*. 2007;578(pt 1):43–53. doi: 10.1113/jphysiol.2006.118745
29. Skrzypiec-Spring M, Grotthus B, Szeląg A, Schulz R. Isolated heart perfusion according to Langendorff—Still viable in the new millennium. *J Pharmacol Toxicol*. 2007;55:113–126. doi: 10.1016/j.vascn.2006.05.006
30. Wischmeyer E, Karschin A. Receptor stimulation causes slow inhibition of IRK1 inwardly rectifying K+ channels by direct protein kinase A-mediated phosphorylation. *Proc Natl Acad Sci U S A*. 1996;93:5819–5823. doi: 10.1073/pnas.93.12.5819
31. Reilly L, Howie J, Wypijewski K, Ashford ML, Hilgemann DW, Fuller W. Palmitoylation of the Na/Ca exchanger cytoplasmic loop controls its inactivation and internalization during stress signaling. *FASEB J*. 2015;29:4532–4543. doi: 10.1096/fj.15-276493
32. Roussel J, Champeroux P, Roy J, Richard S, Fauconnier J, Le Guennec JY, Thireau J. The Complex QT/RR Relationship in Mice. *Sci Rep*. 2016;6:25388. doi: 10.1038/srep25388
33. Speerschneider T, Thomsen MB. Physiology and analysis of the electrocardiographic T wave in mice. *Acta Physiol (Oxf)*. 2013;209:262–271. doi: 10.1111/apha.12172
34. Cerrone M, Noujaim SF, Tolkacheva EG, Talkachou A, O'Connell R, Berenfeld O, Anumonwo J, Pandit SV, Vikstrom K, Napolitano C, et al. Arrhythmogenic mechanisms in a mouse model of catecholaminergic polymorphic ventricular tachycardia. *Circ Res*. 2007;101:1039–1048. doi: 10.1161/CIRCRESAHA.107.148064
35. Panama BK, McLerie M, Lopatin AN. Heterogeneity of IK1 in the mouse heart. *Am J Physiol Heart Circ Physiol*. 2007;293:H3558–H3567. doi: 10.1152/ajpheart.00419.2007
36. Bailie DS, Inoue H, Kaseda S, Ben-David J, Zipes DP. Magnesium suppression of early afterdepolarizations and ventricular tachyarrhythmias induced by cesium in dogs. *Circulation*. 1988;77:1395–1402. doi: 10.1161/01.cir.77.6.1395
37. Brugada P, Wellens HJ. Early afterdepolarizations: role in conduction block, "prolonged repolarization-dependent reexcitation," and tachyarrhythmias in the human heart. *Pacing Clin Electrophysiol*. 1985;8:889–896. doi: 10.1111/j.1540-8159.1985.tb05908.x
38. Edwards AG, Grandi E, Hake JE, Patel S, Li P, Miyamoto S, Omens JH, Heller Brown J, Bers DM, McCulloch AD. Nonequilibrium reactivation of Na+ current drives early afterdepolarizations in mouse ventricle. *Circ Arrhythm Electrophysiol*. 2014;7:1205–1213. doi: 10.1161/CIRCEP.113.001666
39. January CT, Riddle JM, Salata JJ. A model for early afterdepolarizations: induction with the Ca2+ channel agonist Bay K 8644. *Circ Res*. 1988;62:563–571. doi: 10.1161/01.res.62.3.563

40. Hirano Y, Moscucci A, January CT. Direct measurement of L-type Ca2+ window current in heart cells. *Circ Res*. 2018;70:445–455. doi: 10.1161/01.res.70.3.445
41. Pogwizd SM, Onufer JR, Kramer JB, Sobel BE, Corr PB. Induction of delayed afterdepolarizations and triggered activity in canine Purkinje fibers by lysophosphoglycerides. *Circ Res*. 1986;59:416–426. doi: 10.1161/01.res.59.4.416
42. Qu Z, Xie LH, Olcese R, Karagueuzian HS, Chen PS, Garfinkel A, Weiss JN. Early afterdepolarizations in cardiac myocytes: beyond reduced repolarization reserve. *Cardiovasc Res*. 2013;99:6–15. doi: 10.1093/cvr/cvt104
43. Mohamed U, Napolitano C, Priori SG. Molecular and electrophysiological bases of catecholaminergic polymorphic ventricular tachycardia. *J Cardiovasc Electrophysiol*. 2007;18:791–797. doi: 10.1111/j.1540-8167.2007.00766.x
44. Patterson E, Szabo B, Scherlag BJ, Lazzara R. Early and delayed afterdepolarizations associated with cesium chloride-induced arrhythmias in the dog. *J Cardiovasc Pharmacol*. 1990;15:323–331. doi: 10.1097/00005344-199002000-00021
45. Vega AL, Tester DJ, Ackerman MJ, Makielski JC. Protein kinase A-dependent biophysical phenotype for V227F-KCNJ2 mutation in catecholaminergic polymorphic ventricular tachycardia. *Circ Arrhythm Electrophysiol*. 2009;2:540–547. doi: 10.1161/CIRCEP.109.872309
46. Zaza A, Rocchetti M, Brioschi A, Cantadori A, Ferroni A. Dynamic Ca2+-induced inward rectification of K+ current during the ventricular action potential. *Circ Res*. 1998;82:947–956. doi: 10.1161/01.res.82.9.947
47. Burashnikov A, Antzelevitch C. Late-phase 3 EAD. A unique mechanism contributing to initiation of atrial fibrillation. *Pacing Clin Electrophysiol*. 2006;29:290–295. doi: 10.1111/j.1540-8159.2006.00336.x
48. Morotti S, McCulloch AD, Bers DM, Edwards AG, Grandi E. Atrial-selective targeting of arrhythmogenic phase-3 early afterdepolarizations in human myocytes. *J Mol Cell Cardiol*. 2016;96:63–71. doi: 10.1016/j.yjmcc.2015.07.030
49. Said M, Becerra R, Valverde CA, Kaetzel MA, Dedman JR, Mundiña-Weilenmann C, Wehrens XH, Vittone L, Mattiazzi A. Calcium-calmodulin dependent protein kinase II (CaMKII): a main signal responsible for early reperfusion arrhythmias. *J Mol Cell Cardiol*. 2011;51:936–944. doi: 10.1016/j.yjmcc.2011.08.010
50. Thomas G, Gurung IS, Killeen MJ, Hakim P, Goddard CA, Mahaut-Smith MP, Colledge WH, Grace AA, Huang CL-H. Effects of L-type Ca2+ channel antagonism on ventricular arrhythmogenesis in murine hearts containing a modification in the Scn5a gene modelling human long QT syndrome 3. *J Physiology*. 2007;578:85–97. doi: 10.1113/jphysiol.2006.121921
51. Killeen MJ, Gurung IS, Thomas G, Stokoe KS, Grace AA, Huang CL. Separation of early afterdepolarizations from arrhythmogenic substrate in the isolated perfused hypokalaemic murine heart through modifiers of calcium homeostasis. *Acta Physiol (Oxf)*. 2007;191:43–58. doi: 10.1111/j.1748-1716.2007.01715.x
52. Maruyama M, Joung B, Tang L, Shinohara T, On YK, Han S, Choi EK, Kim DH, Shen MJ, Weiss JN, et al. Diastolic intracellular calcium-membrane voltage coupling gain and postshock arrhythmias: role of purkinje fibers and triggered activity. *Circ Res*. 2010;106:399–408. doi: 10.1161/CIRCRESAHA.109.211292
53. Ahlers BA, Zhang XQ, Moorman JR, Rothblum LI, Carl LL, Song J, Wang J, Geddis LM, Tucker AL, Mounsey JP, et al. Identification of an endogenous inhibitor of the cardiac Na+/Ca2+ exchanger, phospholemman. *J Biol Chem*. 2005;280:19875–19882. doi: 10.1074/jbc.M414703200